International Journal of Fluid Power 11 (2010) No. 2 pp. 43-55

ACCURATE SUB-MILLIMETER SERVO-PNEUMATIC TRACKING USING MODEL REFERENCE ADAPTIVE CONTROL (MRAC)

Yong Zhu[1] and Eric J. Barth[2]

[1]*CSC Advanced Marine Center, Washington, DC 20003, USA*
[2]*Department of Mechanical Engineering – Vanderbilt University, Nashville, Tennessee, USA*
yzhu7@csc.com, eric.j.barth@vanderbilt.edu

Abstract

A model reference adaptive controller (MRAC) for compensating friction and payload uncertainties in a servo-pneumatic actuation system is presented in this paper. A friction model combining viscous and Coulomb friction is formulated within the framework of an adaptive controller. Due to the asymmetric nature of Coulomb friction in pneumatic piston actuators, a bi-directional Coulomb friction model is adopted. An update law is presented to estimate three friction parameters: linear viscous friction, Coulomb friction for positive velocity, and Coulomb friction for negative velocity. The force needed to both overcome the estimated friction forces and to supply the desired pressure-based actuation force to obtain a dynamic model reference position response is then used as the command to a sliding mode force controller. Both the force control loop and the adaptation law are Lyapunov stable by design. To ensure stable interaction between the sliding mode force controller and the adaptive controller, the bandwidth of the parameter update law is designed to be appreciably slower than the force tracking bandwidth. Experimental results are presented showing position tracking with and without an unknown payload disturbance. The steady-state positioning accuracy is shown to be less than 0.05 mm for a 60 mm step input with a rise time of around 200 ms. The tracking accuracy is shown to be within 0.7 mm for a 0.5 Hz sinusoidal position trajectory with an amplitude of 60 mm, and within 1.2 mm for a 1 Hz sinusoidal position trajectory with an amplitude of 60 mm. Both step and sinusoidal inputs are shown to reject a payload disturbance with minimal or no degradation in position or tracking accuracy. The control law generates smooth valve commands with a low amount of valve chatter.

Keywords: pneumatic actuation, servo-control, adaptive control

1 Introduction

Adaptive control is a popular method of controlling a dynamic system with uncertainties or slowly changing parameters. Friction and payload are among the most common uncertainties in mechanical systems.

Although pneumatic actuators are highly nonlinear due to the compressibility of air, they often provide a better alternative to electric or hydraulic systems for some applications, such as assembly tasks, which typically require the system to work in a constrained environment (Zhu and Barth, 2005). However, accurate motion control or contact force control is often difficult to achieve with pneumatic actuation and it is therefore typically used only for point to point motions. Accurate closed loop control of pneumatic systems requires adequate dynamic characterization and control. Much progress has been made regarding nonlinear control methodologies for pneumatic systems. Nonlinear lumped parameter models of the compressibility of air and compressible gas flow through control valves have shown a great deal of success in their inclusion in nonlinear model-based control techniques. However, friction and changing inertial loads are often either neglected or assumed fixed. In pneumatic actuators, friction comes mainly from the sliding contact of the piston and rod seals. Friction and load mass have a direct impact on the dynamics of the system in all regimes of operation and can adversely affect accurate control of such systems. In particular, friction has a dominant influence on position control performance especially when the system is operating close to zero velocity. Generally, the direct measurement and *a priori* dynamic characterization of friction is not straightforward and therefore difficult to include effectively in a model-based control scheme. An adaptive friction compensation method will be proposed here to overcome this difficulty.

This manuscript was received on 23 July 2009 and was accepted after revision for publication on 25 June 2010

The method proposed will be shown to compensate not only for friction effects, but will also accommodate changing inertial loads and provide gravity compensation.

Regarding friction modeling and compensation, Armstrong and Canudas de Wit (1996) proposed several static and dynamic friction models. Direct and indirect adaptive controls for friction compensation were also discussed for general dynamic systems. Three adaptive controllers for a permanent magnet linear synchronous motor position control system were proposed in (Liu et al., 2004), including a backstepping adaptive controller, a self-tuning adaptive controller and a model reference adaptive controller. The position control performance of this paper was compared with their work on motor systems, and it will be shown that pneumatic actuators can provide as accurate position control as such electric systems. In the discussion that follows, tracking accuracies are stated but it should be stated that a direct comparison of these across the widely different platforms they were achieved on should be taken lighly.

Although a pneumatic system can possess an inherently low stiffness appropriate for contact and assembly tasks, and can have appealing direct drive capabilities, relatively little work regarding adaptive friction compensation in pneumatic systems for precision control has been done. Wang et al. (Wang et al., 1999) proposed a modified PID controller for a servo pneumatic actuator system where a time delay minimization and target position compensation algorithm was used to achieve accurate position control. The position accuracy was shown to be within 1 mm. An experimental comparison between six different control algorithms including PID, fuzzy, PID with pressure feedback, fuzzy with pressure feedback, sliding mode and neuro-fuzzy control were presented in (Chillari et al., 2001), but none of them focused on the accuracy of position control. Aziz and Bone (1998) proposed an automatic tuning method for accurate position control of pneumatic actuators by combining offline model-based analysis with online iteration. The steady state error accuracy was 0.2 mm with overshoot existing in the step response. A high steady-state accuracy pneumatic servo positioning system was proposed by Ning and Bone (2002) using PVA/PV control and friction compensation. Although the steady state error could be minimized as small as 0.01mm, the system was based on the manual tuning of PVA parameters, and a "good" parameter combination can easily generate large overshoot, or even jeopardize the stability of the system. The system also had a relatively long rise time. In (Karpenko and Sepehri, 2001), a nonlinear position controller for a pneumatic actuator with friction was proposed, and a nonlinear modification to the designed PI controller was introduced. Regulating errors less than 1 mm were achieved consistently. However, when the commanded reference signal was increased to cover up to 60 % of the actuator stroke, the maximum steady state error increased to 4 mm. In (Smaoui et al., 2006) a combined backstepping and sliding mode control approach achieved steady-state tracking errors of 0.1mm but had a high amount of valve chatter. In (Girin et al., 2009) a high-order sliding mode approach achieved steady-state errors as low as 0.01 mm, but again displayed appreciable valve chatter. Although significantly different in control effort and difficult to compare, accurate position control of a pneumatic actuator was also carried out using on/off solenoid valves by Varseveld and Bone (1997). Although often mentioned and discussed, all previous work mentioned above does not *explicitly* consider a friction model in their controller formulations. By considering such a model explicitly, the work presented in this paper achieves accurate control with little valve chatter.

Accurate position control of a pneumatic system (servo-pneumatic control) using a proportional valve will be presented in this work. The proposed controller has a partitioned control structure as shown in Fig. 1. The force control loop deals with the highly nonlinear dynamics of compressed air in the actuator chambers and compressible mass flow through the valves using a sliding mode controller to achieve the desired actuation force. The other loop provides the desired actuation force to the force control loop using an MRAC structure to adaptively compensate for structured friction and payload uncertainties. Inherent in the MRAC structure is a parameterized model of both viscous and Coulomb friction. By combining adaptive control with a robust sliding mode control approach, the work here achieves accurate and smooth control.

The rest of this paper is organized as follows. In Section 2, the friction model will be first presented. In Section 3, the sliding mode force controller will be proposed and experimental results will be presented in Section 5 to show the fast and accurate force tracking up to 30 Hz. In Section 4, a model reference adaptive controller (MRAC) will be designed to estimate the friction parameters and achieve accurate position tracking. In Section 5, experimental results will be presented to show the accurate position control performance, and the ability to accommodate payload uncertainty, of the adaptive controller coupled with the sliding mode force tracking controller. Section 6 contains the concluding remarks.

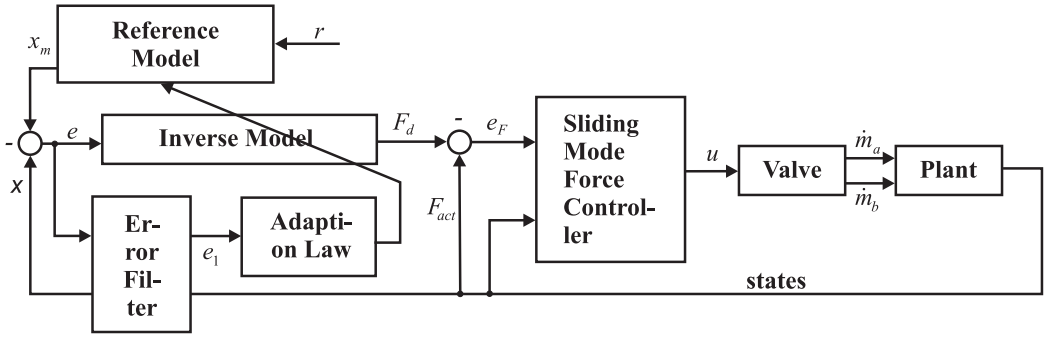

Fig. 1: *Model Reference Adaptive Control (MRAC) structure for accurate pneumatic position tracking.*

2 Friction Model

In order to offer model-based friction compensation and achieve accurate position control, a reasonably accurate and implementable friction model needs to be chosen first. Although friction occurs in almost all mechanical systems, there is no universal friction model applicable to all systems given that the mechanisms of friction are a collection of a number of more fundamental surface interaction and fluid related physical phenomena. For different systems and control objectives, different friction models are adopted to emphasize the regimes and mechanisms of friction most dominant or having the most impact on the chosen objective. A simple Gaussian exponential static friction model, represented in Eq. 1, is often chosen. This description of friction is a function of instantaneous sliding velocity $v(t)$ and captures three friction phenomena: Coulomb, viscous and Stribeck friction.

$$F[v(t)] = F_c \operatorname{sgn}[v(t)] + F_s e^{-[v(t)/v_s]^2} \operatorname{sgn}(v(t)) + F_v v(t) \quad (1)$$

where F_c is the Coulomb friction, F_s is the magnitude of Stribeck friction, v_s is the characteristic velocity of Stribeck friction, and F_v is the linear viscous friction coefficient. By choosing different parameters, different friction models can be realized. This is an adequate model for describing the zero velocity friction force. Figure 2a shows how friction force may evolve continuously from the static friction level. The Stribeck effect is most pronounced very close to zero velocity. Therefore, it is very difficult to capture it using an adaptive law due to the lack of consistent excitation around zero velocity. A simpler friction model including only Coulomb friction and viscous friction, as shown in Fig. 2b, will be used in this work for adaptive friction compensation of a pneumatic actuation system. It will be seen in the experimental results that the tracking performance achieves a high degree of accuracy utilizing this simplified friction model. Because the Coulomb friction in pneumatic actuation systems can be non-symmetric with respect to direction due to the piston and rod seal geometries, it is represented here by two parameters for positive and negative direction, respectively. Therefore, the total friction force F_f that points in a direction opposite of motion is modeled as,

$$F_f[v(t)] = F_v v(t) + F_{cpos} sat1[\operatorname{sgn}(v(t))] + F_{cneg} sat2[\operatorname{sgn}(v(t))] \quad (2)$$

where F_v is the viscous friction parameter, and F_{cpos} and F_{cneg} are the positive and negative direction Coulomb friction force magnitudes. The functions $sat1(\cdot)$ and $sat2(\cdot)$ capture the positive and negative direction velocity information, respectively. When combined with the signum function, positive and negative motion is captured according to the following definitions:

$$sat1[\operatorname{sgn}(v(t))] = \begin{cases} 1 & \text{for } v(t) > 0 \\ 0 & \text{for } v(t) \le 0 \end{cases} \quad (3)$$

$$sat2[\operatorname{sgn}(v(t))] = \begin{cases} -1 & \text{for } v(t) < 0 \\ 0 & \text{for } v(t) \ge 0 \end{cases} \quad (4)$$

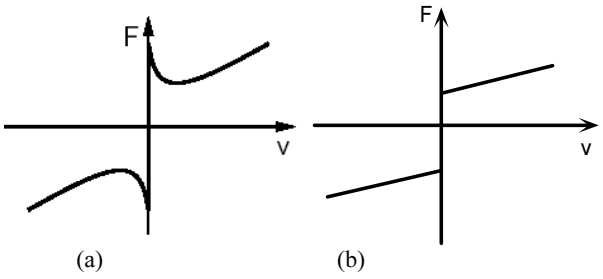

Fig. 2: *Friction models. (a) with Stribeck effect and (b) without Stribeck effect.*

3 Sliding Mode Force Controller

Sliding mode control can maintain robust stability and good performance for nonlinear control systems with modeling inaccuracies. Such a structure provides a good fit for pneumatic control systems given the complexity of the dynamics occurring within, including the nonlinear pressure dynamics and nonlinear mass flow rates through control valves. The force provided by a double-sided, single rod linear pneumatic actuator with pressures P_a and P_b in each side of the cylinder acting on their respective areas A_a and A_b, along with atmospheric pressure P_{atm} acting on the area of the rod $A_r = A_a - A_b$, can be represented as:

$$F_{act} = P_a A_a - P_b A_b - P_{atm} A_r \quad (5)$$

This force will hereby be referred to as the "actuation force". This actuation force will be treated as the controllable input to a single degree of freedom pneumatic actuation system. The strategy will be to specify F_{act} in a manner that both compensates the friction forces in the system while also contributing the correct amount of force for accurate position tracking. Before deriving the control law that will specify the actuation force needed, the ability to track an arbitrary commanded actuation force must first be established. The high bandwidth control of the actuation force is addressed in this section, while the desired actuation force required for accurate position tracking is addressed in the following section.

In order to relate the actuation force to the control valve inputs, taking the derivative of Eq. 5 yields,

$$\dot{F}_{act} = \dot{P}_a A_a - \dot{P}_b A_b \quad (6)$$

For a perfect gas, the rate of change of pressure within each pneumatic chamber of the actuator can be expressed as (Richer and Hurmuzlu, 2000):

$$\dot{P}_{(a,b)} = \frac{\gamma RT}{V_{(a,b)}} \dot{m}_{(a,b)} - \frac{\gamma P_{(a,b)} \dot{V}_{(a,b)}}{V_{(a,b)}} \quad (7)$$

where γ is the thermal characteristic coefficient, with $\gamma = 1$ for isothermal case and γ equaling the ratio of specific heats for the adiabatic case, R is the ideal gas constant, T is the temperature, V is the control volume, and P is the pressure inside each chamber a and b of the pneumatic actuator. The nonlinear relationship between the valve orifice area and the signed net mass flow rate into each chamber using a 4-way proportional valve is given by:

$$\dot{m}_a = A_v \Psi_a(P_u, P_d) \tag{8}$$

$$\dot{m}_b = -A_v \Psi_b(P_u, P_d) \tag{9}$$

where A_v is the high-bandwidth controlled orifice area of the valve and $\Psi(P_u, P_d)$ is the area normalized mass flow rate relationship as a function of the pressure upstream and downstream across each flow channel of the valve. By virtue of the physical arrangement of the valve, the driving pressures of $\Psi(P_u, P_d)$, and ultimately the sign of the mass flow rate, are dependent on the sign of the valve's orifice "area". The convention used here will be that a positive area A_v indicates that the spool of the proportional valve is positioned such that a flow orifice of area A_v connects the high pressure pneumatic supply to one side of the pneumatic cylinder, and thereby promotes a positive mass flow rate into the cylinder chamber. A negative area A_v indicates that the spool of the proportional valve is positioned such that an orifice of area A_v connects one side of the pneumatic cylinder to atmospheric pressure, and thereby promotes a negative mass flow rate (exhaust from the cylinder chamber). The areas of the two flow paths to ports *a* and *b* are then equal and opposite by virtue of the four-way valve design. Using this convention, the area normalized mass flow rate can be written as:

$$\Psi(P_u, P_d) = \begin{cases} \Psi(P_s, P) & \text{for } A \geq 0 \\ \Psi(P, P_{atm}) & \text{for } A < 0 \end{cases} \tag{10}$$

A common mass flow rate model used for compressible gas flowing through a valve is given by (Richer and Hurmuzlu, 2000),

$$\Psi(P_u, P_d) = \begin{cases} \dfrac{C_1 C_f P_u}{\sqrt{T}} & \text{if } \dfrac{P_d}{P_u} \leq C_r \text{ (choked)} \\ \dfrac{C_2 C_f P_u}{\sqrt{T}} \left(\dfrac{P_d}{P_u}\right)^{1/k} \sqrt{1 - \left(\dfrac{P_d}{P_u}\right)^{(k-1)/k}} & \text{otherwise (unchoked)} \end{cases} \tag{11}$$

where P_u and P_d are the upstream and downstream pressures, C_f is the discharge coefficient of the valve, k is the ratio of specific heats, C_r is the pressure ratio that divides the flow regimes into choked and unchoked flow and C_1 and C_2 are constants defined as:

$$C_1 = \sqrt{\frac{k}{R}\left(\frac{2}{k+1}\right)^{(k+1)/(k-1)}} \quad \text{and} \quad C_2 = \sqrt{\frac{2k}{R(k-1)}} \tag{12}$$

The objective of the actuation force controller is to make the actuation force F_{act} track a desired force trajectory F_d (to be specified later). The actuation force tracking error is defined as $e_F = F_{act} - F_d$. It can be seen from Eq. 6 to 9 that $\dot{F}_{act}$ is directly related to the control input $u = A_v$ through the pressure dynamics. Therefore, the dynamic model of the pneumatic actuator force control is a first order nonlinear system if the dynamics of the valve spool position control is neglected (i.e. the bandwidth of the spool valve position control is much higher than the desired force control bandwidth). By combining Eq. 6 to 12, this single input dynamic system can be put into standard functional form as:

$$\dot{F}_{act} = f(P_{a,b}, V_{a,b}, \dot{V}_{a,b}) + b(P_{a,b}, V_{a,b})u \tag{13}$$

where $u = A_v$. The standard time varying sliding surface used in sliding mode control theory (Slotine and Li, 1991) is defined as $s = \left(\frac{d}{dt} + \lambda\right)^{n-1} e$. For a first order system where $n = 1$, s simply becomes:

$$s = e_F = F_{act} - F_d = P_a A_a - P_b A_b - P_{atm} A_r - F_d \tag{14}$$

Taking the time derivative of s and substituting Eq. 7 into $\dot{s}$ yields the sliding mode equation:

$$\dot{s} = \left(\frac{RT}{V_a}\dot{m}_a - \frac{P_a \dot{V}_a}{V_a}\right) A_a - \left(\frac{RT}{V_b}\dot{m}_b - \frac{P_b \dot{V}_b}{V_b}\right) A_b - \dot{F}_d \tag{15}$$

Equating Eq. 14 to zero and substituting Eq. 8 and 9 into Eq. 14 to solve for the equivalent control law gives:

$$u_{eq} = \frac{(P_a A_a^2 V_b + P_b A_b^2 V_a)\dot{x} + V_a V_b \dot{F}_d}{RT[A_a V_b \Psi_a(P_u, P_d) + A_b V_a \Psi_b(P_u, P_d)]} \tag{16}$$

where $\dot{x} = \dot{V}_a / A_a = -\dot{V}_b / A_b$ relating the actuator's chamber volumes to the rod position x.

A discontinuous robustness term is then added across the sliding surface to achieve the typical sliding mode control law:

$$u = u_{eq} - \kappa sat\left(\frac{s}{\varphi}\right) = u_{eq} - \kappa sat\left(\frac{e_F}{\varphi}\right) \tag{17}$$

where κ and ϕ are positive constants that specify the boundary layer (Slotine and Li, 1991). This control law can be easily proven to be Lyapunov stable.

4 Design of a MRAC for Adaptive Friction Compensation

A model reference adaptive controller is designed for friction compensation in this section. The friction parameters F_v, F_{cpos} and F_{cneg} will be estimated by the adaption law and then utilized to derive the appropriate desired actuation force F_d to make the actuator rod position x track a desired trajectory. The choice of a set of model parameters to be estimated adaptively must be uniquely determinable from the model. The open loop dynamics of the pneumatic cylinder are represented according to the following model:

$$\begin{aligned} F_{act} = {} & M\ddot{x} - Mg\cos\theta + \\ & F_v \dot{x} + F_{cpos} sat1[\text{sgn}(\dot{x})] + F_{cneg} sat2[\text{sgn}(\dot{x})] \end{aligned} \tag{18}$$

where θ represents the actuator's angular deviation from a vertical orientation. Although it would appear at first that the mass M should be included in the set of parameters to be estimated, it will be shown that it appears as a common factor that simply scale the friction parameters.

Also not obvious from looking at the model of Eq. 18 is the fact that a constant force offset from gravity, if the piston is oriented with a component aligned with gravity, is able to be encoded using the asymmetric Coulomb friction parameters F_{cpos} and F_{cneg}. The inherent estimation of the inertia and gravity offset will be demonstrated.

An important lesson that was learned from initially choosing only one Coulomb friction parameter, representing a symmetric Coulomb friction model, was that the

adaptive controller will not able to successfully minimize the position tracking error. The Coulomb friction of a typical double-acting, single-rod, pneumatic actuator is asymmetric. Therefore, if the position errors in the positive and negative directions are mixed together as the error information used to adaptively estimate one Coulomb friction parameter, this parameter will not converge but simply "roams" between an upper and lower bound.

In pursuing a model reference adaptive approach, the following reference model was utilized to generate the ideal, or model, dynamic position response $x_m(t)$ to the commanded position signal $r(t)$:

$$\ddot{x}_m + 2\xi\omega_n \dot{x}_m + \omega_n^2 x_m = \omega_n^2 r \tag{19}$$

The desired model-based actuation force, that subsequently becomes the command that is feed into the sliding mode force controller, is chosen as,

$$\begin{aligned} F_d = M(\ddot{x}_m + k_v\dot{e} + k_p e) - Mg\cos\theta + \\ \hat{F}_v\dot{x} + \hat{F}_{cpos}\,sat1[\mathrm{sgn}(\dot{x})] + \hat{F}_{cneg}\,sat2[\mathrm{sgn}(\dot{x})] \end{aligned} \tag{20}$$

where the position error is given by $e = x_m - x$. Control gains k_v and k_p are positive constants chosen to reflect the desired performance specifications in tracking the reference model. Friction parameter estimates are given by $\hat{F}_v$, $\hat{F}_{cpos}$ and $\hat{F}_{cneg}$. Combining Eq. 18 and 20 gives:

$$\begin{aligned} &M\ddot{x} + F_v\dot{x} + F_{cpos}\,sat1[\mathrm{sgn}(\dot{x})] + F_{cneg}\,sat2[\mathrm{sgn}(\dot{x})] = \\ &M(\ddot{x}_m + k_v\dot{e} + k_p e) + \hat{F}_v\dot{x} + \\ &\hat{F}_{cpos}\,sat1[\mathrm{sgn}(\dot{x})] + \hat{F}_{cneg}\,sat2[\mathrm{sgn}(\dot{x})] \end{aligned} \tag{21}$$

subtracting $M\ddot{x}$ from both sides of Eq. 21 yields:

$$\begin{aligned} &F_v\dot{x} + F_{cpos}\,sat1[\mathrm{sgn}(\dot{x})] + F_{cneg}\,sat2[\mathrm{sgn}(\dot{x})] = \\ &M[(\ddot{x}_m - \ddot{x}) + k_v\dot{e} + k_p e] + \hat{F}_v\dot{x} + \\ &\hat{F}_{cpos}\,sat1[\mathrm{sgn}(\dot{x})] + \hat{F}_{cneg}\,sat2[\mathrm{sgn}(\dot{x})] \end{aligned} \tag{22}$$

since $\ddot{x}_m - \ddot{x} = \ddot{e}$, Eq. 22 can be rearranged as:

$$\begin{aligned} &\ddot{e} + k_v\dot{e} + k_p e = \\ &M^{-1}[(F_v - \hat{F}_v)\dot{x} + (F_{cpos} - \hat{F}_{cpos})\,sat1[\mathrm{sgn}(\dot{x})] \\ &+(F_{cneg} - \hat{F}_{cneg})\,sat2[\mathrm{sgn}(\dot{x})]] \end{aligned} \tag{23}$$

Note that M appears as a common factor of the friction parameters in Eq. 23. This fact enables the adaptive estimation of the friction parameters to also include an inherent estimation of the actuator's inertia given that it represents a constant scaling of the friction parameters.

Equation 23 can be rewritten in matrix form as:

$$\begin{aligned} &\ddot{e} + k_v\dot{e} + k_p e = \\ &M^{-1}\underbrace{\begin{bmatrix}\dot{x} & sat1[\mathrm{sgn}(\dot{x})] & sat2[\mathrm{sgn}(\dot{x})]\end{bmatrix}}_{H}\underbrace{\begin{bmatrix}F_v - \hat{F}_v \\ F_{cpos} - \hat{F}_{cpos} \\ F_{cneg} - \hat{F}_{cneg}\end{bmatrix}}_{\tilde{a}} \end{aligned} \tag{24}$$

Defining H and $\tilde{a}$ as above, Eq. 24 can be written more compactly as:

$$\ddot{e} + k_v\dot{e} + k_p e = M^{-1}H\tilde{a} \tag{25}$$

Equation 25 can be represented in the Laplace domain as (note that this s is not the same as the sliding surface s):

$$e(s) = \frac{1}{s^2 + k_v s + k_p} M^{-1}H\tilde{a} \tag{26}$$

A filtered error signal is defined as: $e_1(s) = (s + \eta)e(s)$ (expressed in Laplace domain), where η is a positive constant. The role of e_1 will be to preserve the strictly positive real property of the transfer function relating the estimated signal $M^{-1}H\tilde{a}$ to the error signal used for the adaption. Substituting Eq. 26 into $e_1(s)$ gives this filtered error signal:

$$e_1(s) = \frac{s + \eta}{s^2 + k_v s + k_p} M^{-1}H\tilde{a} \tag{27}$$

Equation 27 forms the basis of the adaptive controller. Eq. 27 can be rewritten in state space form (with e_1 as the output):

$$\dot{X} = AX + BM^{-1}H\tilde{a} \tag{28}$$

$$e_1 = CX \tag{29}$$

where $X = \begin{bmatrix} e \\ \dot{e} \end{bmatrix}$, $A = \begin{bmatrix} 0 & 1 \\ -k_p & -k_v \end{bmatrix}$, $B = \begin{bmatrix} 0 \\ 1 \end{bmatrix}$ and $C = [\eta \quad 1]$.

Based on the Kalman-Yakubovich lemma (Slotine and Li, 1991), since the transfer function $h(s) = C[sI - A]^{-1}B = (s + \eta)/(s^2 + k_v s + k_p) > 0$ is strictly positive real for an appropriate choice of η, k_v and k_p, there exist two symmetric positive definite constant matrices P and Q for the system shown in Eq. 28 and 29, such that $A^TP + PA = -Q$ and $PB = C^T$. A Lyapunov function candidate can be chosen as the following equation according to a standard form to stabilize the system:

$$V(X, \tilde{a}) = X^T PX + \tilde{a}^T\Gamma^{-1}\tilde{a} \tag{30}$$

where $\Gamma = diag(\gamma_1, \gamma_2, \gamma_3)$, $\gamma_i \geq 0$ (i = 1,2,3,), which is also a symmetric positive definite constant matrix. Taking the time derivative of V gives:

$$\dot{V}(X, \tilde{a}) = \dot{X}^T PX + X^T P\dot{X} + \dot{\tilde{a}}^T\Gamma^{-1}\tilde{a} + \tilde{a}^T\Gamma^{-1}\dot{\tilde{a}} \tag{31}$$

Since both $X^TP\dot{X}$ and $\tilde{a}^T\Gamma^{-1}\dot{\tilde{a}}$ are 1×1 matrices, $\dot{X}^TPX = X^TP\dot{X}$ and $\dot{\tilde{a}}^T\Gamma^{-1}\tilde{a} = \tilde{a}^T\Gamma^{-1}\dot{\tilde{a}}$, Eq. 29 can be simplified as:

$$\dot{V}(X, \tilde{a}) = 2\dot{X}^TPX + 2\tilde{a}^T\Gamma^{-1}\dot{\tilde{a}} \tag{32}$$

Substituting Eq. 28 into Eq. 32, along with the fact that PA is symmetric, $A^TP = PA$, and $B^TP = C$, gives,

$$\dot{V}(X, \tilde{a}) = -X^TQX + 2\tilde{a}^T(H^TM^{-1}e_1 + \Gamma^{-1}\dot{\tilde{a}}) \tag{33}$$

If we choose $\dot{\tilde{a}} = -\Gamma H^TM^{-1}e_1$ to eliminate the second term, then $\dot{V}(X, \tilde{a}) = -X^TQX \leq 0$ and ensures stability since Q is positive definite by the Kalman-Yakubovich lemma. Further, since

$$\tilde{a} = \begin{bmatrix} F_{\mathrm{v}} - \hat{F}_{\mathrm{v}} \\ F_{\mathrm{cpos}} - \hat{F}_{\mathrm{cpos}} \\ F_{\mathrm{cneg}} - \hat{F}_{\mathrm{cneg}} \end{bmatrix} = \underbrace{\begin{bmatrix} F_{\mathrm{v}} \\ F_{\mathrm{cpos}} \\ F_{\mathrm{cneg}} \end{bmatrix}}_{p} - \underbrace{\begin{bmatrix} \hat{F}_{\mathrm{v}} \\ \hat{F}_{\mathrm{cpos}} \\ \hat{F}_{\mathrm{cneg}} \end{bmatrix}}_{\hat{p}} = p - \hat{p} \qquad (34)$$

taking the time derivative of Eq. 34 yields $\dot{\tilde{a}} = -\dot{\hat{p}}$. The following adaption law results:

$$\begin{aligned} \dot{\hat{p}} &= \Gamma H^T M^{-1} e_1 \\ &= diag(\gamma_1, \gamma_2, \gamma_3) \begin{bmatrix} \dot{x} \\ sat1[\mathrm{sgn}(\dot{x})] \\ sat2[\mathrm{sgn}(\dot{x})] \end{bmatrix} M^{-1} e_1 \end{aligned} \qquad (35)$$

Equation 35 can be simplified as:

$$\begin{bmatrix} \dot{\hat{F}}_{\mathrm{v}} \\ \dot{\hat{F}}_{\mathrm{cpos}} \\ \dot{\hat{F}}_{\mathrm{cneg}} \end{bmatrix} = \begin{bmatrix} \gamma_1 \dot{x} \\ \gamma_2 sat1[\mathrm{sgn}(\dot{x})] \\ \gamma_3 sat2[\mathrm{sgn}(\dot{x})] \end{bmatrix} M^{-1} e_1 \qquad (36)$$

Equation 36 is the update law for the estimation of the friction parameters. The standard derivation is based on Lyapunov stability theory.

5 Experimental Results

Experiments were conducted to show 1) high bandwidth force tracking using the sliding mode force controller, and 2) accurate step and sinusoidal position tracking with adaptive friction compensation. A photograph of the experimental setup is shown in Fig. 3.

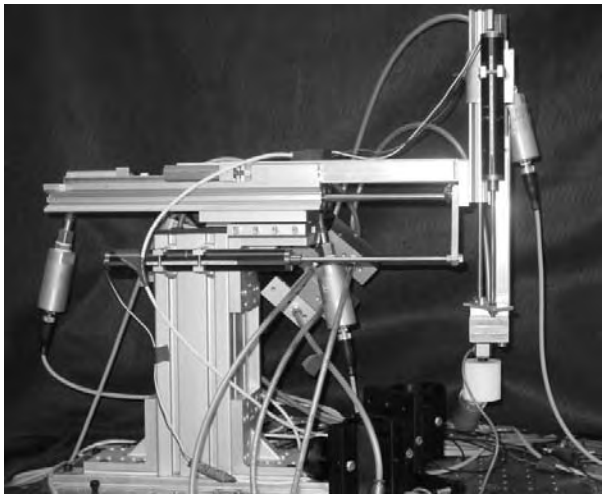

Fig. 3: *The experimental setup of the pneumatic actuation servo system.*

The pneumatic manipulator is based on a Festo two degree-of-freedom pick and place pneumatic system. The position tracking experiments are carried out using the vertical direction double acting pneumatic cylinder (SLT-16-100-P-A), which has a stroke length of 100 mm. A linear potentiometer (Midori LP-100F) with 100 mm maximum travel is used to measure the linear position of the vertical cylinder. The velocity was obtained from position by utilizing an analog differentiating filter with a 20 dB roll-off at 33 Hz. The acceleration signal was obtained from the velocity signal with a digital differentiating filter with a 20 dB roll-off at 30 Hz. One four-way proportional valve (Festo MPYE-5-M5-010-B) is attached to the two chambers of the vertical cylinder. Two pressure transducers (Festo SDE-16-10V/20mA) are attached to each cylinder chamber, respectively. Control is provided by a computer with one A/D board (National Instruments PCI-6031E) with analog input channels for the sensors, and another A/D board (Measurement Computing PCIM-DDA06/16) with analog output channels to control the proportional valves. The middle point of the cylinder stroke is defined as the zero position.

In the experiments, the following parameters were used:

Table 1: General Parameters:

Description	Symbol	Value
Supply Pressure	P_{s}	652.2 kPa
Atm. Pressure	P_{atm}	101 kPa
Nominal Inertia	M	1.05 kg
Piston Area	A_{a}	402.12 mm^2
Piston Area	A_{b}	345.58 mm^2
Rod Areas	A_{r}	56.54 mm^2
Ratio of specific Heats	k	1.4
Mass flow constant	C_1	4.0418×10^5
Mass flow constant	C_2	1.5617×10^4
Pressure ratio	C_{r}	0.528
Discharge Coeff	C_{f}	0.2939
Specific Gas Constant	R	287 J/kg/K
Amb. Temperature	T	300 K

Table 2: Sliding Mode Force Controller:

Description	Symbol	Value
Robustness gain	κ	4.3 mm^2/mN
Boundary layer	ϕ	26000 mN

Table 3: Adaptive Controller:

Description	Symbol	Value
Ref Model Nat. Freq	ω_{n}	40 rad/sec
Ref Model Damp. Ratio	ξ	1
Tracking damping	k_{v}	200 rad/sec
Tracking stiffness	k_{p}	4000 rad/sec^2
Error filter zero	η	30 rad/sec
Adaption scaling	γ_1	0.01 kg^2/mm/sec
Adaption scaling	γ_2	50 kg^2/sec
Adaption scaling	γ_3	50 kg^2/sec

The sliding mode force controller was implemented using Eq. 17 which computes the signed valve orifice area $u = A_{\mathrm{v}}$ based on the force error $e_{\mathrm{F}} = F_{\mathrm{act}}\ F_{\mathrm{d}}$ and the equivalent control expression of Eq. 16. The model reference adaptive controller generated the appropriate force command signal for the sliding mode force controller through Eq. 20 where the position error was

computed as $e = x_m - x$ with the model position response $x_m(t)$ computed from Eq. 19 based on the commanded position r. The adaptive friction parameters of Eq. 20 were updated using Eq. 36 which utilizes the filtered error signal computed as $e_1(s) = (s + \eta)e(s)$.

5.1 Sliding Mode Force Controller Performance

The actuation force tracking performance of the sliding mode force controller for 1 Hz and 20 Hz sinusoidal inputs is shown in Fig. 4. Up to 30 Hz (188 rad/sec), the valve and controller can still provide good force tracking. In these experiments, the cylinder rod is fixed at the middle stroke position.

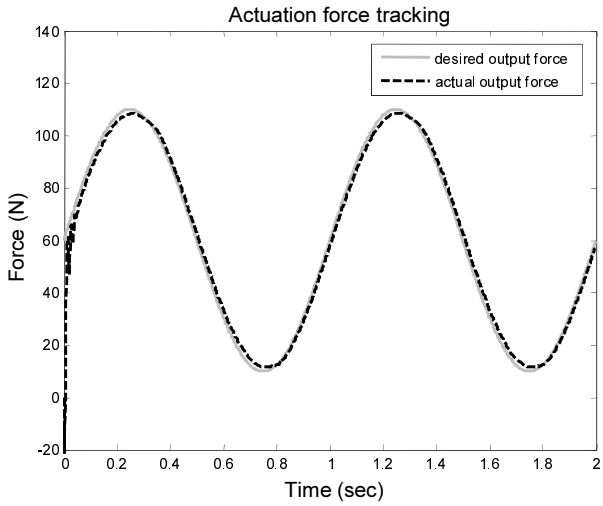

(a) 1 Hz actuation force tracking

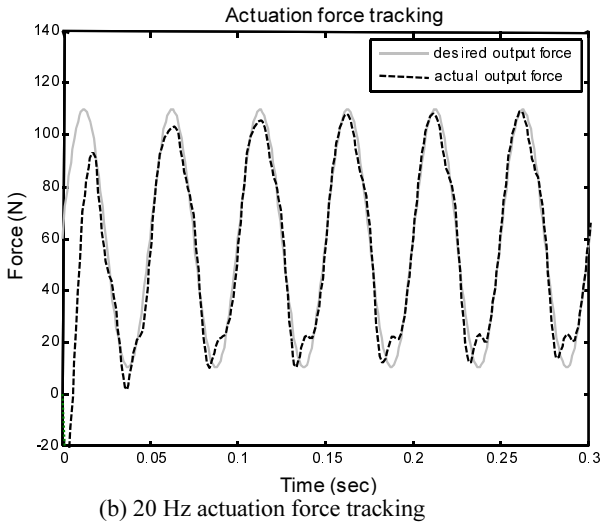

(b) 20 Hz actuation force tracking

Fig. 4: *Experimental results of the sliding mode controller actuator force tracking for sinusoidal input with frequency: (a) 1 Hz and (b) 20 Hz.*

5.2 MRAC Controller Performance

Step tracking of 60 mm amplitude is presented in Fig. 5. The moving mass of the vertical cylinder was 0.67 kg and a 0.38 kg mass was attached to it as a payload. It can be seen that the adaptive friction compensation can effectively compensate the unmodeled changes in friction behavior induced by the change in amplitude. The parameters all converge quickly. The steady state error of the step response is within 0.05 mm. A close inspection of the steady-state error reveals that the accuracy is as good as perhaps 0.035 mm; a spectral analysis of the error signal reveals distinct peaks at 60 Hz and 180 Hz suggesting noise from electrical power and not actual displacement in steady-state. The rise time (10 % to 90 %) is about 200 ms for step inputs from -30 mm to 30 mm. The valve command shows little chatter. It is conjectured that the combined feed forward aspects offered by the parameters estimated by the adaptive portion of the controller, combined with a boundary-layer sliding mode controller, allows for smooth control inputs to the plant.

Sinusoidal tracking of 0.5 Hz and 1 Hz with a 60 mm amplitude are presented in Fig. 6 and 7. It can be seen that the adaptive friction compensation can effectively compensate for unmodeled changes in friction behavior at different velocities. For the 0.5 Hz sinusoidal input, the tracking error is within 0.7 mm. For the 1 Hz sinusoidal input, the tracking error is within 1.2 mm.

In all tracking cases, the higher bandwidth of the sliding mode force tracking controller (greater than 188 rad/sec) relative to the parameter adaption (at 30 rad/sec), along with the fact that sliding mode control offers a robust control approach, ensures stable interaction between the force tracking dynamics and the adaptive controller.

5.2.1 60mm Step Tracking

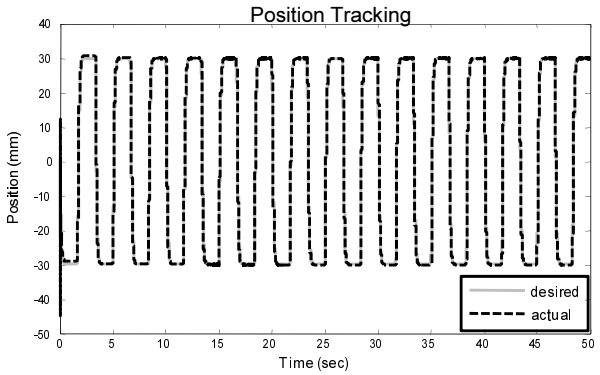

(a) 60 mm step tracking

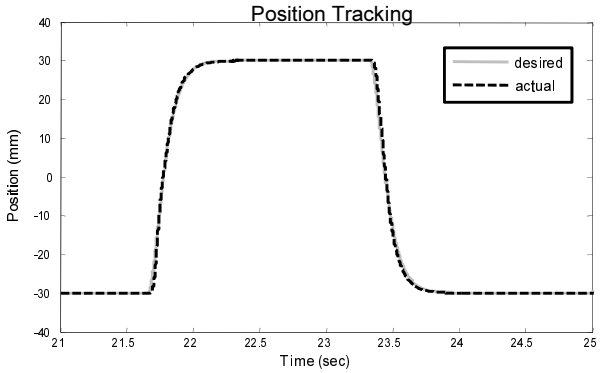

(b) Zoom in time showing the shape of the reference model response to a step input and the MRAC controller's performance in tracking it

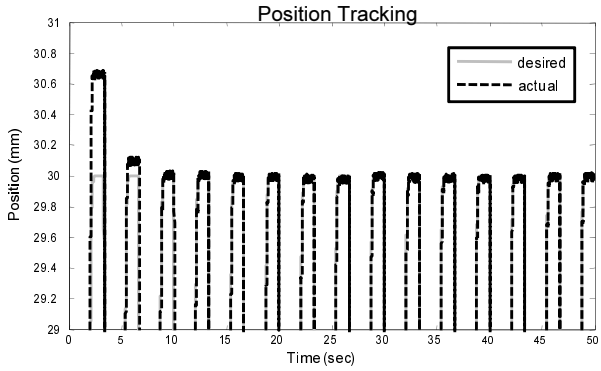

(c) Zoom of 60 mm step tracking precision at top

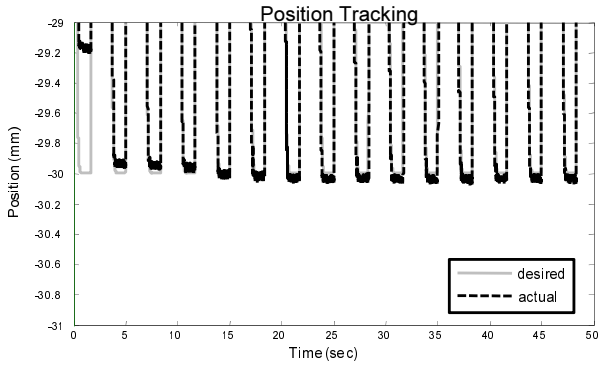

(d) Zoom of 60 mm step tracking precision at bottom

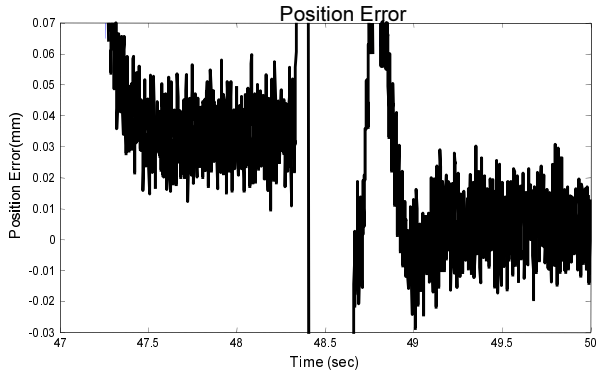

(e) Zoom of steady-state error

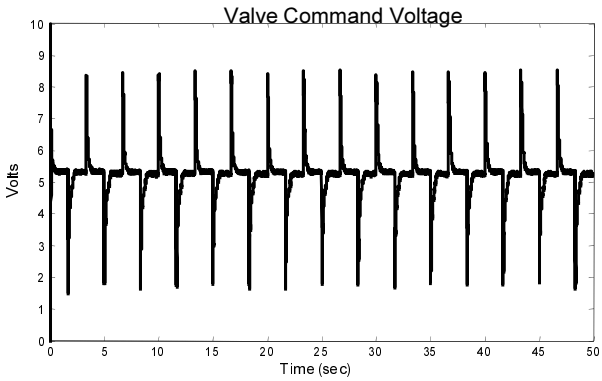

(f) Valve input voltage

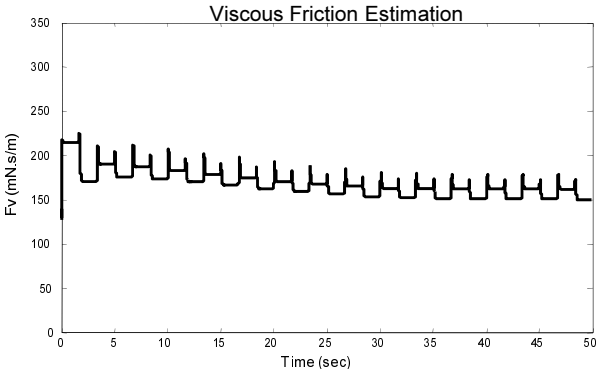

(g) Viscous friction parameter estimation

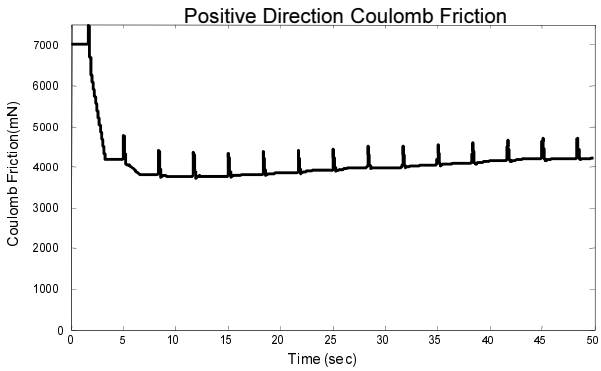

(h) Positive direction Coulomb friction estimation

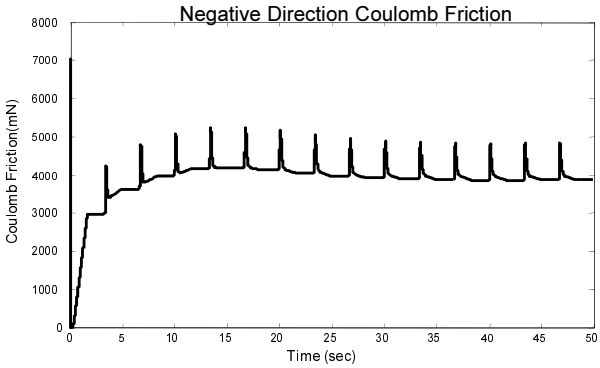

(i) Negative direction Coulomb friction estimation

Fig. 5: *60mm step response. (a) position tracking, (b) zoom in of one step showing reference model response and actual response, (c) upper side steady state error, (d) lower side steady state error, (e) zoom of steady-state error, (f) valve control command, (g) viscous friction estimation, (h) positive direction Coulomb friction estimation and (i) negative direction Coulomb friction estimation.*

5.2.2 60mm Sinusoidal Tracking at 0.5 Hz

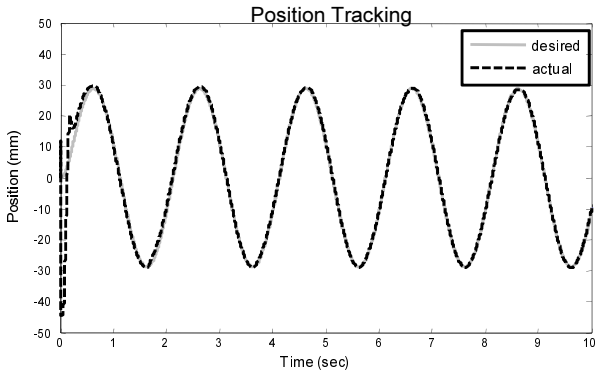

(a) 0.5 Hz sinusoidal tracking

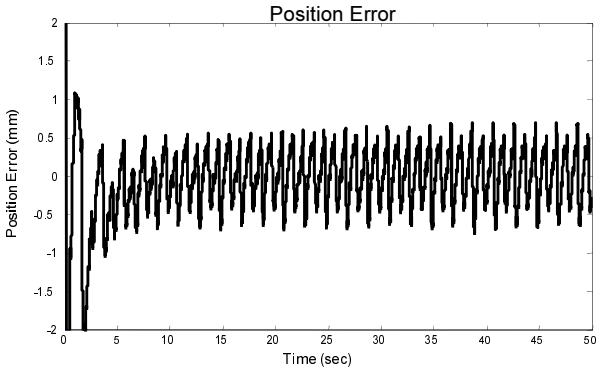

(b) Position tracking error

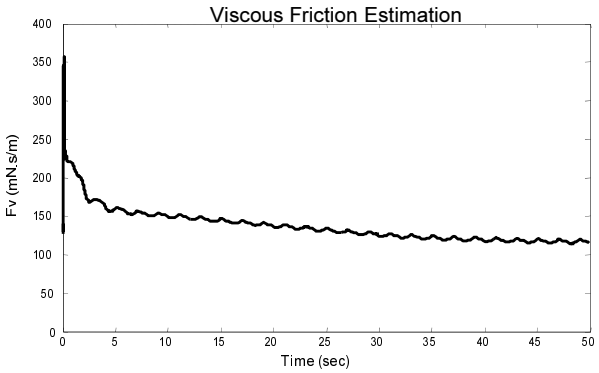

(c) Viscous friction parameter estimation

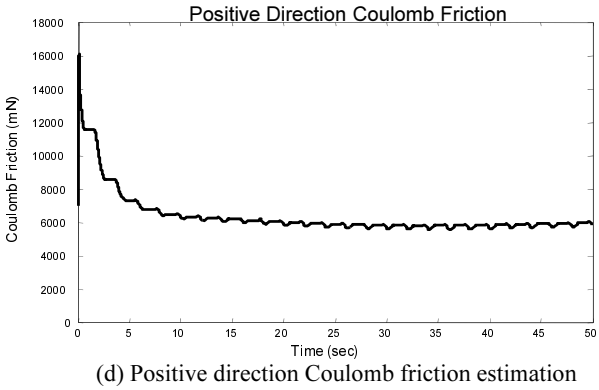

(d) Positive direction Coulomb friction estimation

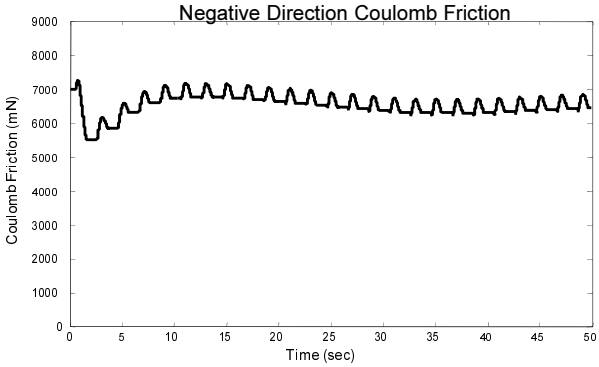

(e) Negative direction Coulomb friction estimation

Fig. 6: *0.5 Hz 60mm sinusoidal tracking. (a) position tracking, (b) position error, (c) viscous friction estimation, (d) positive direction Coulomb friction estimation and (e) negative direction Coulomb friction estimation.*

5.2.3 60mm Sinusoidal Tracking at 1 Hz

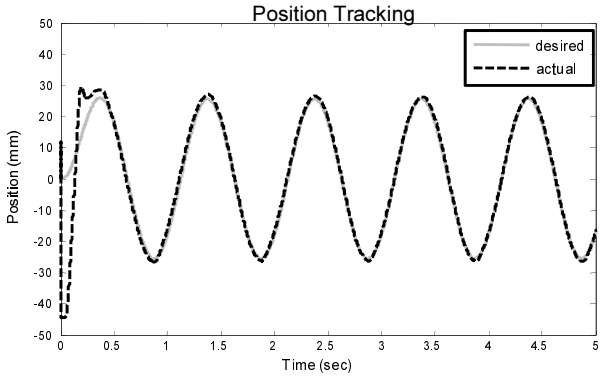

(a) 1 Hz sinusoidal tracking

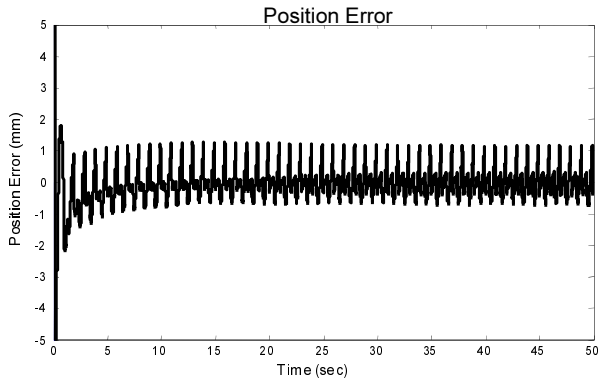

(b) Position tracking error

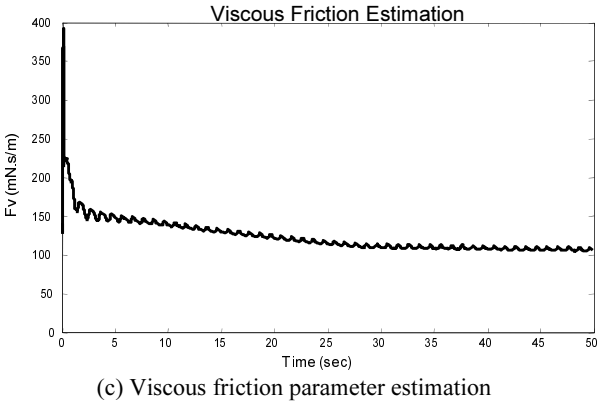

(c) Viscous friction parameter estimation

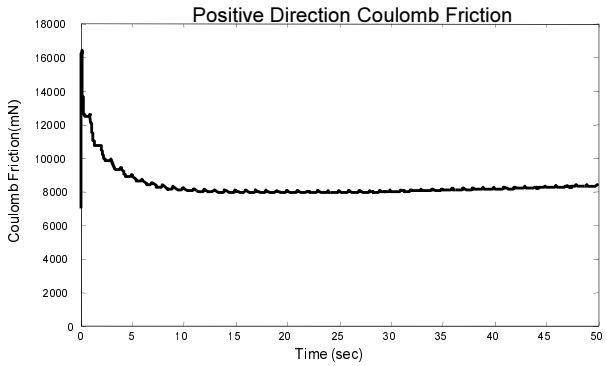

(d) Positive direction Coulomb friction estimation

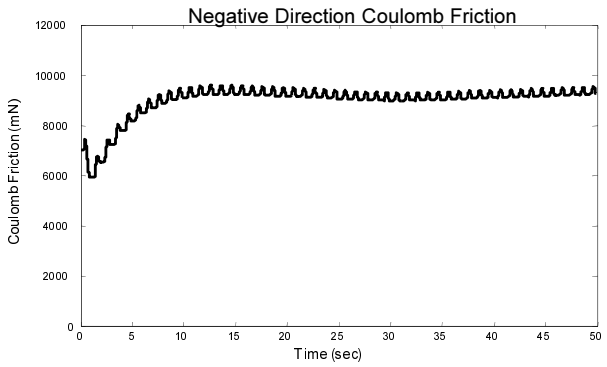

(e) Negative direction Coulomb friction estimation

Fig. 7: *1 Hz 60mm sinusoidal tracking. (a) position tracking, (b) position error, (c) viscous friction estimation, (d) positive direction Coulomb friction estimation and (e) negative direction Coulomb friction estimation.*

5.3 MRAC Controller Performance with Unmodeled Payload Disturbance

Figures 8 and 9 show that the system can well accommodate a payload disturbance and still maintain accurate position control for both step and sinusoidal inputs. To represent an unknown or varying payload, the moving mass was changed from 1.05 kg to 1.78 kg by assuming that the end effector grasps a 0.73 kg part. Therefore an unmodeled gravitational force of 7.15 N was present, but the gravity compensation of Eq. 20 was still using a modeled mass of M = 1.05 kg. Experimental results show that the adaptive model-based controller can compensate this unmodeled gravitational force offset, as well as compensating for the unmodeled increase in inertia. Comparing Fig. 5g with Fig. 8f, it can be seen that the positive direction Coulomb friction has changed from 4.2 N to – 2.9 N. The difference is 7.1 N, which is very close to the unmodeled static force offset due to gravity. Comparing Fig. 5h with Fig. 8g, it can be seen that the negative direction Coulomb friction has changed from 4.1 N to 11.2 N. The difference is again 7.1 N. The adaptive Coulomb compensation accurately compensates the offset of gravity and changes in inertia while maintaining good position tracking performance. The steady state error with payload disturbance is within 0.1 mm.

Less obvious is the adaptive payload compensation during sinusoidal tracking – here the friction parameters have also changed to account for the unmodeled static force difference. Also less obvious in both step tracking and sinusoidal tracking is the fact that the change in inertia has been compensated to maintain accurate tracking.

5.3.1 60mm Step Tracking with Payload Disturbance

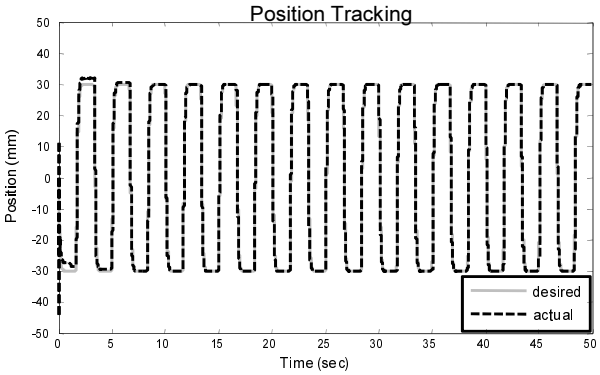

(a) 60 mm step tracking with payload disturbance

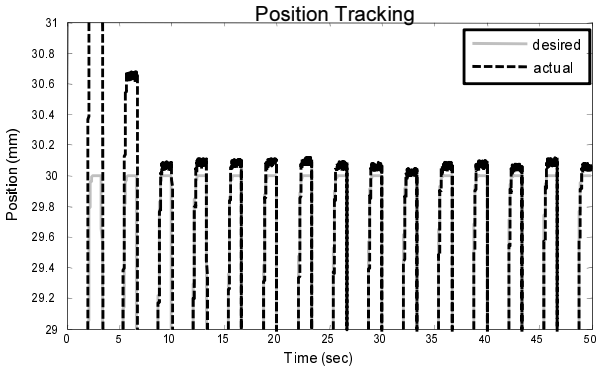

(b) Zoom of 60 mm step tracking precision at top

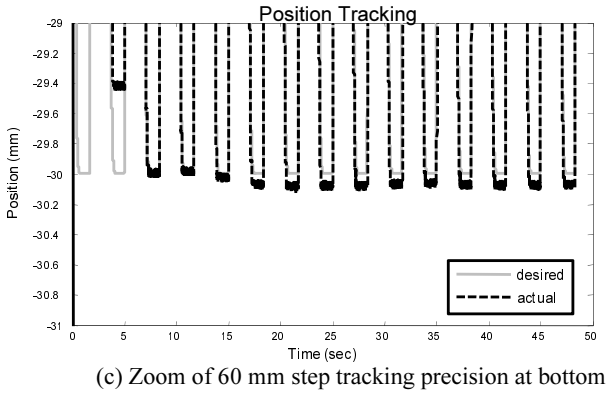

(c) Zoom of 60 mm step tracking precision at bottom

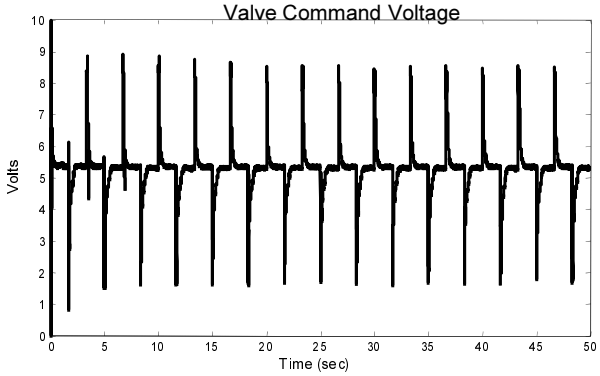

(d) Valve input voltage

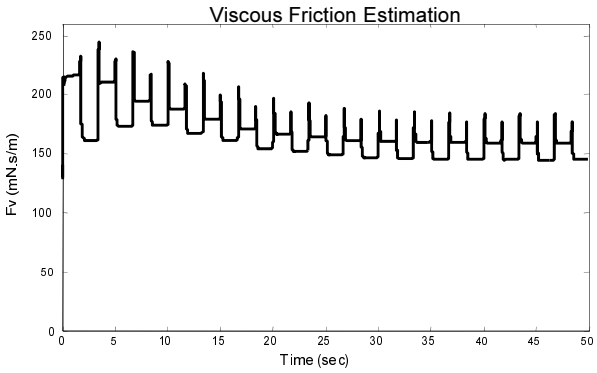

(e) Viscous friction parameter estimation

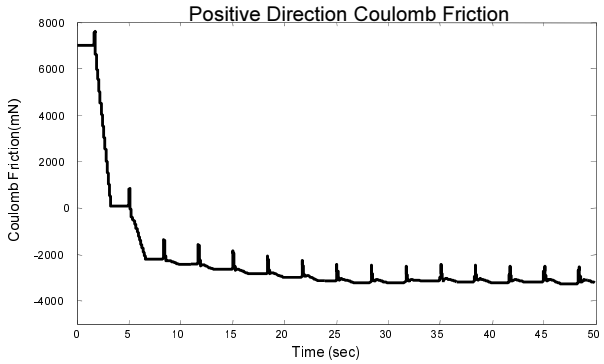

(f) Positive direction Coulomb friction estimation

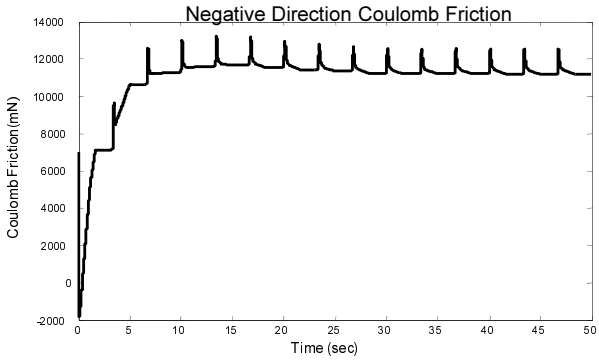

(g) Negative direction Coulomb friction estimation

Fig. 8: *60mm step tracking with model mass error. (a) position tracking, (b) upper side steady state error, (c) lower side steady state error, (d) valve control command, (e) viscous friction estimation, (f) positive direction Coulomb friction estimation and (g) negative direction Coulomb friction estimation.*

5.3.2 60mm Sinusoidal Tracking at 0.5 Hz with Payload Disturbance

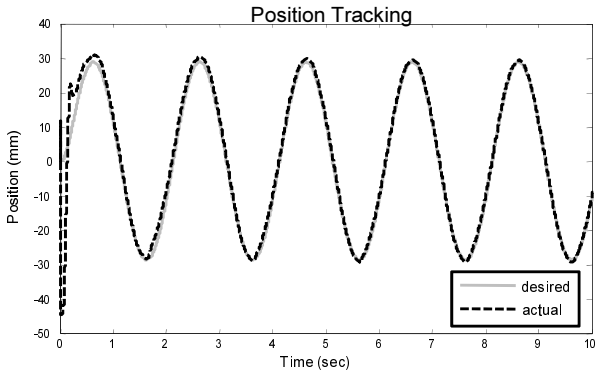

(a) 0.5 Hz sinusoidal tracking with payload disturbance

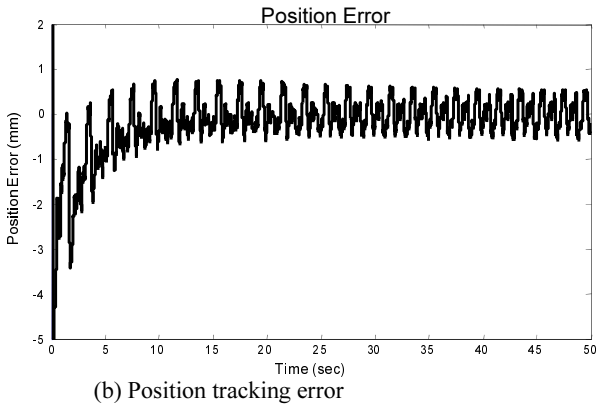

(b) Position tracking error

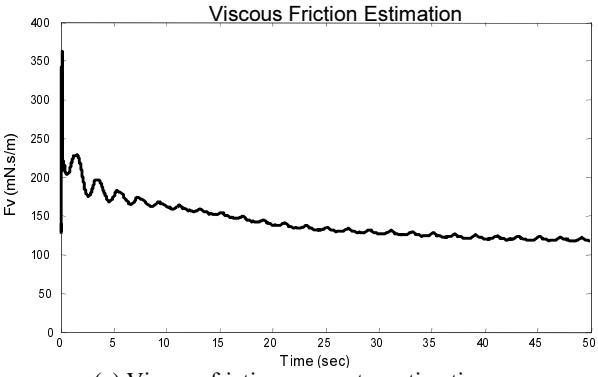

(c) Viscous friction parameter estimation

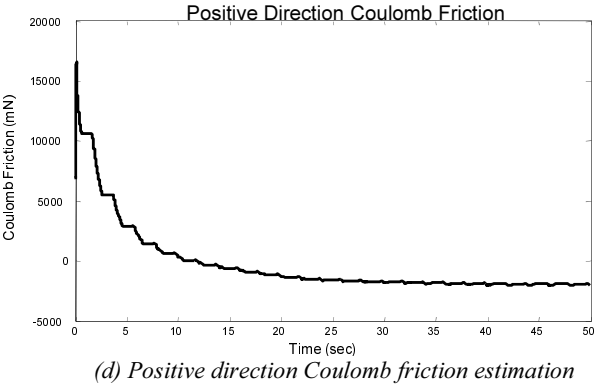

(d) Positive direction Coulomb friction estimation

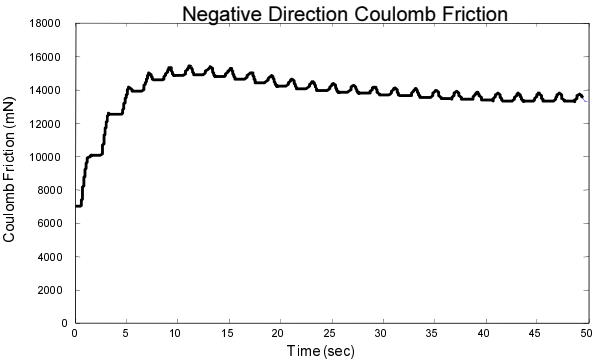

(e) Negative direction Coulomb friction estimation

Fig. 9: *1 Hz 60mm sinusoidal tracking with model mass error. (a) position tracking, (b) position error, (c) viscous friction estimation, (d) positive direction Coulomb friction estimation and (e) negative direction Coulomb friction estimation.*

6 Conclusions

Accurate position control in free space for pneumatic actuators is achieved using model reference adaptive control to specify the required actuation force, and sliding mode control to achieve high-bandwidth actuation force tracking. The position control performance and adaptive parameter convergence are comparable to electric motor systems. The system can well adapt to inputs of different magnitudes and frequency content maintaining fine position tracking. The adaptive friction structure proposed can also compensate for the error generated by unmodeled inertial and gravitational forces associated with payload uncertainty. Finally, it is conjectured that the steady-state positioning accuracy of the proposed method is capable of even higher fidelity than that shown here given that it was limited by the resolution and noise of the position sensing used in this work and not by the method itself.

Nomenclature

F_c	Coulomb friction	[N]
F_s	Stribeck friction magnitude	[N]
F_v	Viscous friction parameter	[N·s/m]
F_f	Total friction force	[N]
F_{cpos}	Positive direction Coulomb friction	[N]
F_{cneg}	Negative direction Coulomb friction	[N]
$sat1(\cdot)$	Positive saturation function	[N]
$sat2(\cdot)$	Negative saturation function	[N]
$P_{(a,b)}$	Actuator pressures (side a, b)	[Pa]
P_{atm}	Atmospheric pressure	[Pa]
$A_{(a,b)}$	Actuator areas (side a, b)	[m^2]
A_r	Actuator rod area	[m^2]
F_{act}	Actuation force	[N]
γ	Polytropic constant	[-]
R	Ideal gas constant	[kJ/kg/K]
T	Temperature	[K]
$V_{(a,b)}$	Actuator chamber volume (side a, b)	[m^3]
$\dot{m}_{(a,b)}$	Mass flow (in/out side a, b)	[kg/s]
$A\nu$	Signed valve orifice area	[m^2]
P_u	Upstream pressure	[Pa]
P_d	Downstream pressure	[Pa]
k	Ratio of specific heats	[-]
C_f	Valve discharge coefficient	[-]
C_r	Critical pressure ratio	[-]
F_d	Desired actuation force	[N]
u	Valve control input	[m^3]
e_F	Force tracking error	[N]
u_{eq}	Equivalent control component	[m^3]
κ	Sliding mode robustness gain	[m^2/N]
ϕ	Sliding mode boundary layer	[N]
M	Actuator/load inertia	[kg]
r	Reference model input	[m]
x_m	Reference model response	[m]
ω_n	Reference model natural frequency	[rad/s]
ξ	Reference model damping ratio	[-]
e	Position error	[m]
k_v	Tracking damping parameter (gain)	[rad/s]
k_p	Tracking stiffness parameter (gain)	[rad/s^2]
$\underset{\sim}{a}$	Adaptive parameter vector	[-]
H	Adaptive signal matrix	[-]
η	Error filter zero location	[rad/s]
$\gamma_{(1,2,3)}$	Adaption scaling	[-]
P	Lyapunov equation matrix	[-]
Q	Lyapunov equation matrix	[-]

References

Armstrong, B. and **Canudas de Wit, C.** 1996. Friction Modeling and Compensation, *The Control Handbook* (by William S. Levine), CRC Press, pp. 1369-1382.

Aziz, S. and **Bone, G. M.** 1998. Automatic Tuning of an Accurate Position Controller for Pneumatic Actuators, *Proceedings of the 1998 IEEE/RSJ International Conference on Intelligent Robots and Systems*, pp.1782-1788.

Chillari, S., **Guccione, S.** and **Muscato, G.** 2001. An Experimental Comparison between Several Pneumatic Position Control Methods, *Proceedings of the 2001 IEEE Conference on Decision and Control*, pp. 1168-1173.

Girin, A., **Plestan, F.**, **Brun, X.**, and **Glumineau, A.** 2009. High-Order Sliding-Mode Controllers of an Electropneumatic Actuator: Application to an Aeronautic Benchmark, *IEEE/ASME Transactions on Control Systems Technology*, vol. 17, no. 3, pp. 633-645.

Karpenko, M. and **Sepehri, N.** 2001. Design and Experimental Evaluation of a Nonlinear Position Controller for a Pneumatic Actuator with Friction, *Proceedings of the 2004 American Control Conference*, Boston, MA, pp. 5078-5083.

Liu, T., **Lee, Y.** and **Chang, Y.** 2004. Adaptive Controller Design for a Linear Motor Control System, *IEEE transactions on Aerospace and Electronic Systems*, vol. 40, no. 2, pp. 601-616.

Ning, S. and **Bone, G. M.** 2002. High Steady-state Accuracy Pneumatic Servo Positioning System with PVA/PV Control and Friction Compensation, *Proceedings of the 2002 IEEE International Conference on Robotics and Automation*, pp. 2824-2829.

Richer, E. and **Hurmuzlu, Y.** 2000. A High Performance Pneumatic Force Actuator System: Part I – Nonlinear Mathematical Model, *ASME Journal of Dynamic Systems, Measurement, and Control*, vol. 122, no. 3, pp. 416-425.

Slotine, J. E. and **Li, W.** 1991. *Applied Nonlinear Control*, pp. 338, Prentice Hall.

Smaoui, M., **Brun, X.**, and **Thomasset, D.** 2006. Systematic Control of an Electropneumatic System: Integrator Backstepping and Sliding Mode Control, *IEEE/ASME Transactions on Control Systems Technology*, vol. 14, no. 5, pp. 905-913.

Van Varseveld, R. B. and **Bone, G. M.** 1997. Accurate Position Control of a Pneumatic Actuator Us-

ing On/Off Solenoid Valves, *IEEE/ASME Transactions on Mechatronics*, vol. 2, no. 3, pp. 195-204.

Wang, J., **Pu, J.** and **Moore, P.** 1999. Accurate Position Control of Servo Pneumatic Actuator Systems: an Application for Food Packaging, *Control Engineering Practice*, vol. 7, pp. 699-706.

Zhu, Y. and **Barth, E. J.** 2005. Planar Peg-in-hole Insertion Using a Stiffness Controllable Pneumatic Manipulator, *Proceedings of the 2005 International Mechanical Engineering Congress and Exposition*.

Eric J. Barth
received the B.S. degree in engineering physics from the University of California at Berkeley, and the M.S. and Ph.D. degrees from the Georgia Institute of Technology in mechanical engineering in 1994, 1996, and 2000 respectively. He is currently an Associate Professor of Mechanical Engineering at Vanderbilt University. His research interests include design, modeling and control of fluid power systems, and actuator development for autonomous robots.

Yong Zhu
received the B.E. degree from Harbin Institute of Technology, Harbin, China, in 1999, the M.S. degree from Northern Illinois University, DeKalb, IL, in 2003, and the Ph.D. degree in mechanical engineering from Vanderbilt University, Nashville, TN, in 2006. He is currently a Mechanical Engineer Leader at CSC Advanced Marine Center, Washington, DC. His current research interests include modeling, simulation and control of dynamic systems and the design and prototyping of electromechanical systems.